High latitude meteoric $\delta^{18}O$ compositions: Paleosol siderite in the Middle Cretaceous Nanushuk Formation, North Slope, Alaska

David F. Ufnar[†]
Department of Geology, University of Southern Mississippi, Box 5044, Hattiesburg, Mississippi 39406, USA

Greg A. Ludvigson[‡]
Iowa Geological Survey Bureau, Iowa City, Iowa 52242, USA and *Center for Global and Regional Environmental Research, University of Iowa, Iowa City, Iowa 52242, USA*

Luis A. González[§]
Department of Geology, University of Kansas, Lawrence, Kansas 66045-7613, USA

Robert L. Brenner[#]
Department of Geoscience, University of Iowa, Iowa City, Iowa 52242-1379, USA

Brian J. Witzke[††]
Iowa Geological Survey Bureau, Iowa City, Iowa 52242, USA

ABSTRACT

Siderite-bearing pedogenic horizons of the Nanushuk Formation of the North Slope, Alaska, provide a critical high paleolatitude oxygen isotopic proxy record of paleoprecipitation, supplying important empirical data needed for paleoclimatic reconstructions and models of "greenhouse-world" precipitation rates. Siderite $\delta^{18}O$ values were determined from four paleosol horizons in the National Petroleum Reserve Alaska (NPR-A) Grandstand # 1 Core, and the values range between −17.6‰ and −14.3‰ (PDB) with standard deviations generally less than 0.6‰ within individual horizons. The $\delta^{13}C$ values are much more variable, ranging from −4.6‰ to +10.8‰ (PDB). A covariant $\delta^{18}O$ versus $\delta^{13}C$ trend in one horizon probably resulted from mixing between modified marine and meteoric phreatic fluids during siderite precipitation.

Groundwater values calculated from siderite oxygen isotopic values and paleobotanical temperature estimates range from −23.0‰ to −19.5‰ (SMOW). Minor element analyses show that the siderites are impure, having enrichments in Ca, Mg, Mn, and Sr. Minor element substitutions and Mg/Fe and Mg/(Ca + Mg) ratios also suggest the influence of marine fluids upon siderite precipitation.

The pedogenic horizons are characterized by gleyed colors, rare root traces, abundant siderite, abundant organic matter, rare clay and silty clay coatings and infillings, some preservation of primary sedimentary stratification, and a lack of ferruginous oxides and mottles. The pedogenic features suggest that these were poorly drained, reducing, hydromorphic soils that developed in coal-bearing delta plain facies and are similar to modern Inceptisols.

Model-derived estimates of precipitation rates for the Late Albian of the North Slope, Alaska (485–626 mm/yr), are consistent with precipitation rates necessary to maintain modern peat-forming environments. This information reinforces the mutual consistency between empirical paleotemperature estimates and isotope mass balance models of the hydrologic cycle and can be used in future global circulation modeling (GCM) experiments of "greenhouse-world" climates to constrain high latitude precipitation rates in simulations of ancient worlds with decreased equator-to-pole temperature gradients.

Keywords: siderite, oxygen isotopes, Cretaceous, paleosols, carbon isotopes, paleoclimatology.

INTRODUCTION

Meteoric $\delta^{18}O$ values for the warm equable middle Cretaceous have been estimated throughout the Western Interior Basin from paleosol sphaerosiderites (Ludvigson et al., 1998; White et al., 2000a, b, 2001; Ufnar et al., 2001, 2002). Pedogenic siderites of the Nanushuk Formation of the North Slope, Alaska, provide a critical high paleolatitude (75°N) meteoric $\delta^{18}O$ proxy record for paleoclimatic reconstructions and models of "greenhouse-world" precipitation rates (Ufnar et al., 2002). The pedogenic siderites of the Nanushuk formed under similar conditions, and are compositionally similar to the sphaerosiderites described by Ludvigson et al. (1998) and Ufnar et al. (2001). The Nanushuk siderites differ only in texture, in that they generally lack the well-developed radial-concentric crystalline microstructure. Here, they are simply referred to as pedogenic siderites.

Sphaerosiderites are millimeter-scale $FeCO_3$ nodules that formed in ancient wetland paleosols. Isotopic analyses from individual sphaerosiderite- and siderite-bearing paleosols and pedogenic horizons often define

[†]E-mail: david.ufnar@usm.edu.
[‡]E-mail: gludvigson@igsb.uiowa.edu.
[§]Present address: Center for Global and Regional Environmental Research, University of Iowa, Iowa City, Iowa 52242, USA; e-mail: lgonzlez@ku.edu.
[#]E-mail: robert-brenner@uiowa.edu.
[††]E-mail: bwitzke@igsb.uiowa.edu.

GSA Bulletin; March/April 2004; v. 116; no. 3/4; p. 000–000; 11 figures; 2 tables.

trends of invariant $\delta^{18}O$ and variable $\delta^{13}C$ values, defined as meteoric sphaerosiderite lines (MSLs) by Ludvigson et al. (1998). The MSLs are analogous to the meteoric calcite lines (MCLs) of Lohmann (1988), substantiate precipitation from meteoric phreatic fluids, and are a proxy for the $\delta^{18}O$ of ancient precipitation.

Middle Cretaceous climatic equability refers to putative decreased annual temperature variations, diminished seasonal temperature extremes, and limited periods of subfreezing temperatures in the polar regions (Sloan and Barron, 1990). There is much evidence for a reduced middle Cretaceous equator-to-pole temperature gradient (Barron and Washington, 1982; Spicer and Corfield, 1992). Empirical evidence for middle Cretaceous polar warmth includes the biogeography of terrestrial plant fossils (Parrish and Spicer, 1988a, b), and the distribution and isotopic composition of marine organisms (Lloyd, 1982; Mutterlose, 1992; Huber et al., 2002). Based upon GCM experiments, Barron et al. (1995) suggested that global temperature gradients are primarily affected by three variables: paleogeography, increased atmospheric CO_2 concentrations, and increased ocean heat flux. The middle Cretaceous paleogeography, which was significantly different from that of today, may have played a major role in reducing meridional temperature gradients and increasing ocean heat transport from the tropics (Barron et al., 1995; Poulsen et al., 1999). The warmest sea surface paleotemperature estimates (SSTs) (26–32 °C) of the last 120 Ma come from Aptian-Albian deposits from equatorial Pacific Deep Sea Drilling Project (DSDP) sites (Douglas and Savin, 1975). Warm SSTs have also been determined for high paleolatitude marine deposits of the middle Cretaceous. Aptian through Albian mean annual temperatures were determined to be 16 °C at 60°S from DSDP site 511 (Huber et al., 1995, 2002), and 10–13 °C in the Late Albian (DSDP site 511) (Fassell and Bralower, 1999).

Fossil leaf physiognomy (Wolfe, 1971, 1979; Wolfe and Upchurch, 1987), particularly leaf-margin analysis of fossils in the Nanushuk Formation, provides empirical terrestrial paleotemperature constraints for the middle Cretaceous of the North Slope, Alaska. Leaf-margin analyses yield mean annual temperatures (MATs) of 10° ± 3 °C (Spicer and Parrish, 1986; Parrish and Spicer, 1988a, b). The abundance of fossil vegetation in the Nanushuk Formation implies that water was plentiful during the middle Cretaceous (Spicer and Parrish, 1986; Parrish and Spicer, 1988a, b); however, quantitative empirical constraints on precipitation rates have not been previously reported.

Proxy records of paleoprecipitation are needed to constrain GCM modeling experiments, as the hydrologic cycle is very sensitive to climatic forcing factors such as atmospheric CO_2 concentrations, tectonics, paleogeography, and orbital variations (Barron et al., 1989). Changes in the Earth's orbit cause changes in the receipt of incoming solar radiation, and the polar regions are especially sensitive to these variations (Harrington, 1987; Schlesinger, 1997). Based upon modeling experiments, Poulsen et al. (1999) concluded that elevated atmospheric CO_2 concentrations (four times present-day concentrations) caused increased precipitation rates at high latitudes. The development of quantitative empirical data from high-latitude regions is imperative for constraining precipitation rates in the ''greenhouse-world'' of the middle Cretaceous and verification of GCM model outputs.

In this paper we show that pedogenic siderites from the middle Cretaceous Nanushuk Formation provide a proxy record of the $\delta^{18}O$ of high-latitude meteoric groundwaters recharged by local paleoprecipitation. Furthermore, based upon isotopic compositions of the pedogenic siderites and modeling results of Ufnar et al. (2002), we show that estimates of middle Cretaceous precipitation rates from coal-bearing strata on the North Slope, Alaska, are consistent with those required for modern peat bog formation.

Geologic Setting

Outcrops of nonmarine Lower and Upper Cretaceous rocks on Alaska's North Slope are comprised of sediments that were deposited between 75° and 85° N paleolatitudes (Spicer and Parrish, 1990a, b) (Fig. 1). Carbonaceous mudstones containing siderite-bearing pedogenic horizons have been identified, providing biostratigraphic and geochemical data for this crucial high-latitude portion of Cretaceous North America. Analyses of plant paleoecology, vegetational and leaf physiognomy, growth rings, and vascular systems in Cretaceous woods from the North Slope, Alaska, by Parrish and Spicer (1988a, b) and Spicer and Parrish (1990a, b) show that climate cooled substantially from the ''middle'' to Late Cretaceous.

Uplift of the present-day Brooks Range during the Cretaceous led to deposition of a thick wedge of siliciclastic sediments on Alaska's North Slope. Surface and subsurface data indicate that up to 10,000 m of sediment were shed into a rapidly subsiding foredeep basin, the Colville Basin, during the late Aptian through the Cenomanian (Mull, 1985). The bulk of non-marine strata are contained in the Nanushuk Group (previous nomenclature), the proximal portion of a major Albian-to-Cenomanian depositional cycle defined by Mull (1985). Deposits of the upper Nanushuk Group in the Umiat area of the Colville Basin reached maximum burial depths (~2 km) and paleotemperatures (60–70 °C) during the early Paleocene (O'Sullivan, 1999). Age relationships are not well established for the Nanushuk Group; however, palynological analyses indicate that most of the Nanushuk Group is Albian in age (Mull, 1985; Molenaar, 1985) (Fig. 2).

Molenaar (1985) interpreted the Nanushuk Group as consisting of deltaic complexes with multiple tongues of marine and nonmarine sandstones and shales. It has been divided into a lower, dominantly marine facies (Kukpowruk Formation in the western portion of the depositional basin, or Grandstand and Tuktu Formation in the east), and an upper dominantly nonmarine facies (Corwin Formation in the west or Chandler Formation in the east). These formal Formation names have recently been abandoned by Mull et al. (2003) (see below). Published descriptions of nonmarine lithologies other than sandstones are highly generalized, mentioning coals, carbonaceous shale, trough cross-bedded conglomerates, and shales, but they include no mention of any structures or lithologies resembling paleosols (Huffman, 1985; Molenaar, 1985; Mull, 1985).

In an effort to improve understanding of the regional lithostratigraphy, Mull et al. (2003) have revised the stratigraphic nomenclature of the Colville Basin. Therein, the Nanushuk Group has been reduced in rank and revised as the Nanushuk Formation. It is generally comprised of two unnamed informal units; the lower is predominantly marine and the upper is nonmarine. The Kukpowruk, Tuktu, Corwin, Chandler, Grandstand, and Ninuluk Formations have all been abandoned (Mull et al., 2003).

The sampled intervals of the Nanushuk Formation in the Grandstand #1 core generally consist of interbedded fine- to medium-grained, cross-bedded sandstones; dark-gray, carbonaceous mudstones; and thin lignitic coal beds (Fig. 3). The lithofacies units represent fluvial-deltaic point bar and crevasse splay deposits (sandstones), pedogenically modified overbank (floodplain) deposits (carbonaceous mudstones), and peat bogs (coals) (Ahlbrandt, 1979; Huffman, 1985).

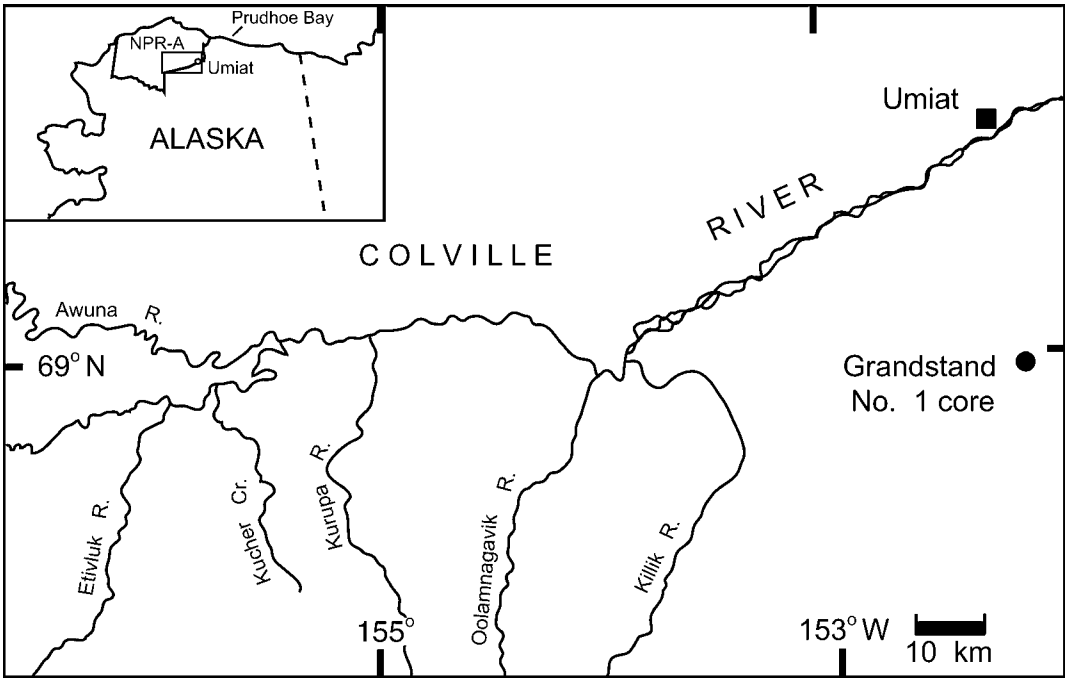

Figure 1. Map of Colville River area in North Slope, Alaska, indicating location of National Petroleum Reserve Grandstand #1 Core (modified from Spicer and Parrish, 1986). R.—river; C.—creek.

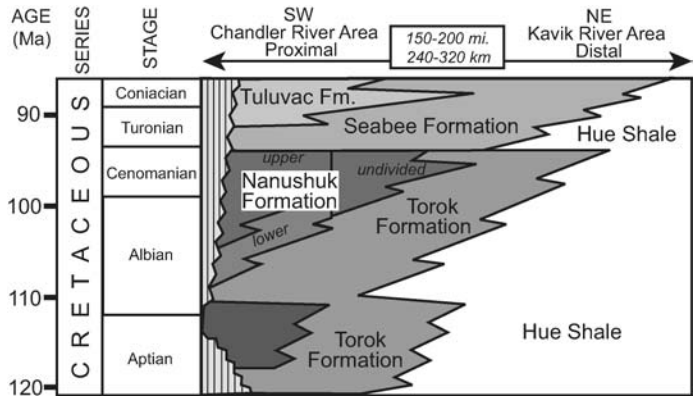

Figure 2. Stratigraphic correlation chart for mid-Cretaceous deposits of the Colville Basin, North Slope, Alaska (modified from Mull et al., 2003). Mbr.—member.

METHODS

Lithologic descriptions and samples were collected from the National Petroleum Reserve (NPR) Grandstand # 1 core stored at the U.S. Geological Survey Core Research Center in Denver, Colorado. The specimens collected are generally only a few centimeters thick, and due to poor recovery in sections of the core, the specimens were named according to the depth in the core from which they were sampled (e.g., 171.34 m). Specimens were vacuum impregnated with epoxy resin and cut to produce doubly polished thin sections and thin slabs for microsampling. Separate core samples of the highly carbonaceous mudstones were collected from the same depth-intervals for palynological analyses. The palynological identifications were performed by Bob Ravn of Aeon Biostratigraphic Services, Anchorage, Alaska.

Pedogenic siderites were evaluated using light microscopy, cathodoluminescence (CL) petrography, epifluorescence petrography, and scanning electron microscopy. These imaging techniques were used to identify all carbonate phases present in the specimens and to delineate suitable domains to be microsampled. Polished slabs from each of the pedogenic horizons were microsampled for carbonates using a microscope-mounted drill assembly with a 0.5 mm drill bit. The powdered samples were treated with dilute acetic acid as an additional precaution to leach trace amounts of calcite and dolomite that may have been present in the microsamples and to ensure complete isolation of siderite for isotopic analyses. All samples extracted for mass spectrometry were analyzed at the University of Iowa, Paul H. Nelson Stable Isotope Laboratory.

Powdered samples were vacuum-roasted at 380 °C to remove volatile contaminants. Samples were then reacted with anhydrous phosphoric acid at 72 °C in an on-line, automated Kiel III carbonate reaction device coupled to the inlet of a Finnigan MAT 252 isotope ratio mass spectrometer. All isotopic values were reported relative to the PeeDee Belemnite (PDB) standard, with analytical precision of better than $\pm 0.05‰$ for carbon and oxygen. Siderite data were corrected with the experimentally determined temperature-dependent isotope fractionation factor of Carothers et al. (1988).

Electron microprobe analyses were conducted on siderites and other carbonate cements from each of the four sampled horizons using a JEOL JXA-8900R electron microprobe at the University of Minnesota. Siderite analyses were performed using wavelength dispersive spectrometry at an accelerating voltage of 15 kV, a beam current of 10 nA,

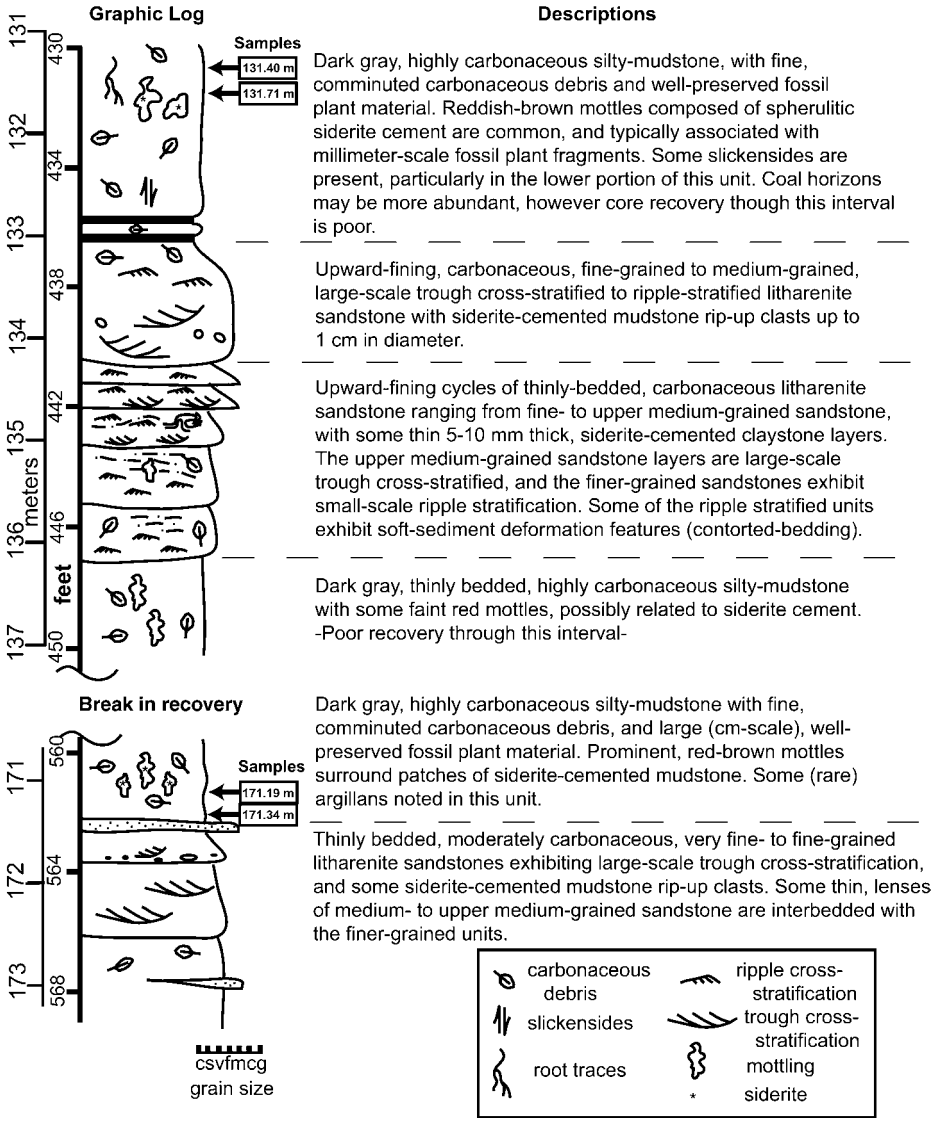

Figure 3. Lithologic log and descriptions of sampled intervals in NPR Grandstand #1 Core. Grandstand core reached a total depth of 1201 m. There are 26 cored intervals totaling 233 m in length. For this study, portions of cored intervals between 126 and 137 m and 171 and 175 m were described and sampled for isotopic analyses. To see specific cored intervals, refer to USGS Core Research Facility, Denver, Colorado, Web site (http://geology.cr.usgs.gov/crc/data/AK/ak-colat.htm).

TABLE 1.

NPR Grandstand #1 Core, 131.4 m, Palynological Species
Bisaccate gymnosperm pollen, indet.
Deltoidospora spp.
Cicatricosisporites venustus
Sabalpollenites sp. - indet.
Cicatricosisporites sp. - indet.
Gleicheniidites senonicus
Cicatricosisporites australiensis
Retitriletes sp. - indet.
Podocarpidites sp. - indet.
Ischyosporites cf. crassimacerius
Foveosporites sp. - indet., triangular, fine
Osmundacidites wellmanii
Laevigatosporites ovatus

Note: indet.—indeterminate.

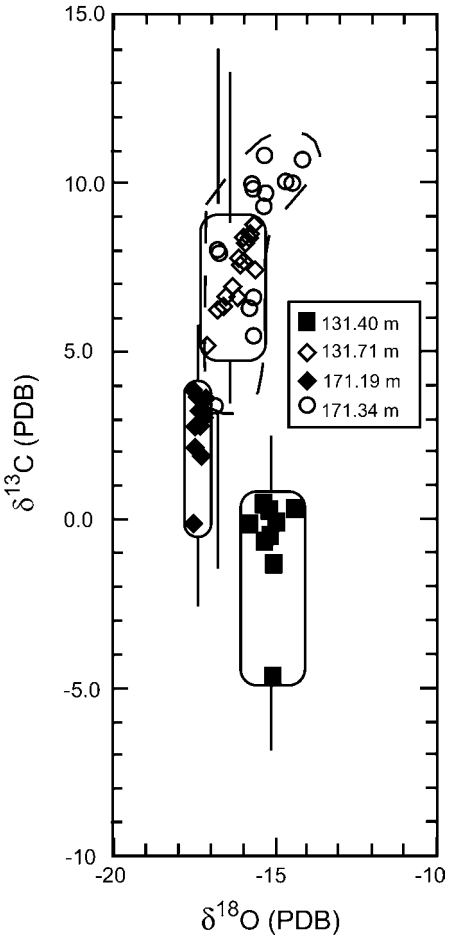

Figure 4. Carbon and oxygen isotopic values of paleosol siderites from 171.34-m, 171.19-m, 131.71-m, and 131.40-m depth intervals of NPR Grandstand #1 Core. Rectangular fields envelope a range of isotopic values for individual horizons, and vertical lines define MSL values.

and a beam diameter of 5 μm. The following x-ray lines and standards were used: $Ca_{K\alpha 1}$ -calcite, $Mg_{K\alpha 1}$ -dolomite, $Mn_{K\alpha 1}$ -rhodonite, $Fe_{K\alpha 1}$ -siderite, and $Sr_{K\alpha 1}$ -strontianite.

RESULTS

Palynostratigraphic Implications

The four depth-intervals sampled from the Grandstand #1 core were generally devoid of recognizable palynomorph species with the exception of the 131.4 m depth interval. The presence of *Cicatricosisporites venustus*, *Cicatricosisporites australiensis* and *Ischyosporites cf. crassimacerius* in the sample from 131.4 m are indicative of a late Albian/early Cenomanian age (Table 1).

Stable Isotopes of Carbon and Oxygen

Four siderite-bearing pedogenic horizons were sampled for isotopic analyses in this study. No fewer than 10 analyses were performed on each unit (Fig. 4). The 171.34 m depth interval has siderite $\delta^{18}O$ values ranging

from −16.84‰ to −14.13‰ (PDB) with a mean of 15.6‰ (std. dev. 0.82‰). The $\delta^{13}C$ values range from +3.38‰ to +10.76‰ (PDB) with a mean of +8.39‰ (std. dev. 2.23‰) (Fig. 4). The 171.19 m depth interval has siderite $\delta^{18}O$ values ranging from −17.56‰ to −17.19‰ (PDB) with a mean of −17.4‰ (std. dev. 0.13‰). The $\delta^{13}C$ values range from −0.15‰ to +3.80‰ (PDB) with a mean of +2.5‰ (std. dev. 1.14‰). The 131.71 m depth interval is characterized by siderite $\delta^{18}O$ values ranging from −17.09‰ to −15.57‰ (PDB) with a mean of −16.2‰ (std. dev. 0.44‰). The $\delta^{13}C$ values range from +5.14‰ to +8.85‰ (PDB) with a mean of 7.35‰ (std. dev. 1.04‰). The 131.40-m depth interval has siderite $\delta^{18}O$ values ranging from −15.84‰ to −14.50‰ (PDB) with a mean of −15.2‰ (std. dev. 0.35‰). The $\delta^{13}C$ values range between −4.63‰ and +0.48‰ (PDB) with a mean of −0.6‰ (std. dev. 1.50‰) (Fig. 4).

Groundwater isotopic compositions were calculated over a range of temperatures (0–25 °C) from the mean siderite $\delta^{18}O$ values and the experimentally determined, temperature-dependent fractionation factor for siderite (Carothers et al., 1988). Based on empirical paleotemperature estimates of Parrish and Spicer (1988a, b), groundwater $\delta^{18}O$ values ranged from −23.0‰ to −19.5‰ (SMOW) (Fig. 5).

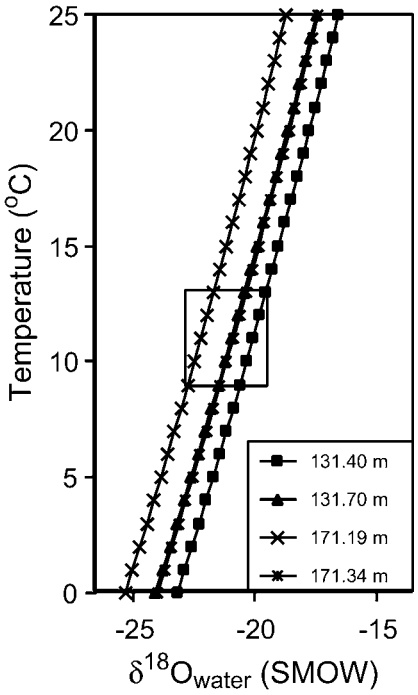

Figure 5. Soil groundwater values calculated from paleosol siderite $\delta^{18}O$ values over a range of temperatures (0–25 °C). Rectangle denotes range of empirical mean annual paleotemperature estimates determined by Parrish and Spicer (1988) for Albian North Slope of Alaska.

Paleosol Micromorphology

General Characteristics

The pedogenic horizons sampled for this study are all gleyed carbonaceous mudstones characterized by an abundance of fine, comminuted coaly debris, and larger (millimeter-scale) fragments of fossilized plant matter. Stipple-speckled, striated, or crystallitic b-fabrics (b = birefringence) are observed. Speckled b-fabrics are characterized by small (<20μm), randomly oriented, equidimensional to slightly elongate patches of optically oriented clays and correspond to Brewer's (1964) insepic and asepic plasmic fabrics (Bullock et al., 1985). Small, generally silt-sized birefringent crystallites or mineral grains characterize crystallitic b-fabrics. Striated b-fabrics (sepic plasmic fabrics of Brewer, 1964) consist of elongate zones of oriented clays in which the particles generally exhibit uniform extinction in cross-polarized light (Bullock et al., 1985).

The primary pedofeatures observed in these units are typic argillaceous and carbonaceous coatings, infillings, and crystalline pedofeatures. Coatings are features that cover the surfaces of voids, grains, and aggregates, and typic indicates they are of consistent thickness (Bullock et al., 1985). Argillaceous coatings are composed of layered, optically oriented clays, and carbonaceous coatings consist of opaque organic material (argillans and organs of Brewer, 1964). Infillings are voids that have been partly or completely filled and differ from coatings in that they are more than 90% filled (Bullock et al., 1985). In paleosols, the difference between coatings and infillings is complicated due to compaction and a decrease of primary porosity. For this study, planar accumulations of clay particles or carbonaceous matter are referred to as coatings, and pods or crescent-shaped, laminated pedofeatures are referred to as infillings. The siderite nodules are typic, crystalline pedofeatures with distinct internal fabrics and sharp boundaries (Bullock et al., 1985). The siderite (nonluminescent in CL) generally occurs in the following forms, all of which may be present in a given unit: (1) Small (10–20 μm) crystallites disseminated throughout the groundmass (Fig. 6A) or densely packed to form pervasively siderite-cemented mudstone domains (Fig. 6B); (2) Aggregates of individual crystallites reorganized to crudely concentric, spherical nodules (50–150 μm in size) (Fig. 6, C and D); and (3) Small (50–150 μm) sphaerosiderites that exhibit characteristic spherulitic crystalline microstructures (Ludvigson et al., 1998) (Fig. 6, E and F). Ferroan dolomite cements exhibiting bright orange-red luminescence are commonly associated with carbonaceous plant fossil fragments (Fig. 6B) and cementing some of the mudstone domains. The dolomitic cements engulf siderite crystallites in the groundmass and fill voids associated with carbonaceous debris. Thus, it is inferred that the dolomite precipitated as a later diagenetic cement, after the siderite. A more detailed description of the groundmass and pedofeatures observed in each of the four sampled pedogenic horizons is summarized in Table 2.

Elemental Analyses

Microprobe analyses of siderite from all four horizons show compositions that are generally greater than 80 mol % $FeCO_3$, with substitutions of Ca^{2+}, Mg^{2+}, Mn^{2+}, and minor amounts of Sr^{2+} (Fig. 7). The 171.34 m depth interval is characterized by siderite compositions ranging from 88.60 to 93.64 mol % $FeCO_3$. Calcium substitution ranges from 2.31 to 3.69 mol % $CaCO_3$, Mg^{2+} ranges from 0.62 to 5.10 mol % $MgCO_3$, and Mn^{2+} ranges from 1.74 to 2.96 mol % $MnCO_3$ (Fig. 8). Substitutions of Sr^{2+} are less than 0.052 mol % $SrCO_3$. The carbonate cement vein filling in the carbonaceous fossil cracks has an intermediate composition in the CaO-MgO-FeO solid solution system (Fig. 7). The cement has a composition that is closest to ferroan dolomite with an average composition of $(Ca_{56.29}, Mg_{28.88}, Fe_{14.45,} Mn_{0.40})CO_3$. The 171.19-m depth interval is characterized by siderite compositions ranging from 83.20 to 88.79 mol % $FeCO_3$ (Fig. 7). Substitutions of Ca^{2+} range from 3.80 to 5.37 mol % $CaCO_3$, Mg^{2+} ranges from 3.86 to 9.99 mol % $MgCO_3$, Mn^{2+} ranges from 1.34 to 2.79 mol % $MnCO_3$, and Sr^{2+} occurs in trace amounts not exceeding 0.03 mol % $SrCO_3$ (Fig. 8). The carbonate cement composition is similar to that of the 171.34 m depth interval, having an average composition of $(Ca_{50.01}, Mg_{34.28}, Fe_{15.30,} Mn_{0.40})CO_3$ (Fig. 7). The 131.71-m depth interval is characterized by siderite compositions ranging from 87.33 to 90.74 mol % $FeCO_3$. Substitutions of Ca^{2+} range from 3.62 to 5.04 mol % $CaCO_3$, Mg^{2+} ranges from 3.67 to 6.17 mol % $MgCO_3$, Mn^{2+} ranges from 1.46 to 1.91 mol % $MnCO_3$, and Sr^{2+} concentrations do not exceed 0.07 mol % $SrCO_3$. The carbonate cement has an average composition of $(Ca_{50.97}, Mg_{33.49}, Fe_{15.24,} Mn_{0.42})CO_3$. The 131.40-m

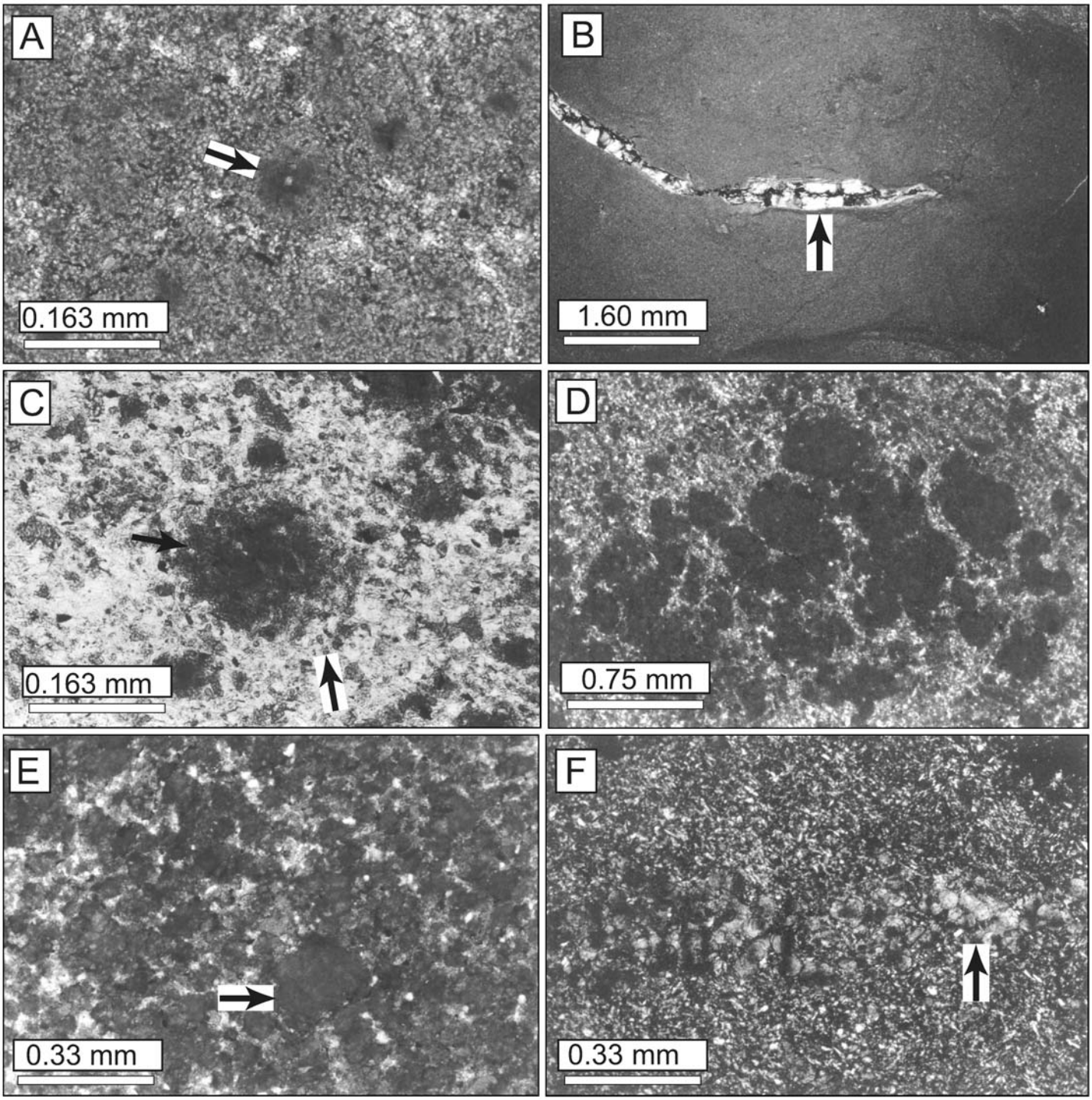

Figure 6. (A) Photomicrograph exhibiting ubiquitous siderite crystallites in paleosol groundmass of 171.34-m depth interval (plane-polarized light, PPL). Arrow points to a dense aggregate of siderite crystallites that are organized into crude nodular form. (B) Arrow points to sparry, ferroan dolomite that was precipitated in a void containing remnant carbonaceous material (black). Background is pervasively cemented with microcrystalline siderite (171.34-m depth interval; cross-polarized light, CPL). (C) Lower arrows point to a single siderite crystallite, and upper arrow points to dense aggregate of crystallites that are organized into crude nodule (171.19-m depth interval; PPL). (D) Cluster of siderite nodules composed of aggregated siderite crystallites (171.19 m depth interval; PPL). (E) Arrow points to siderite crystallites that are organized to a nodule that exhibits crude concentric internal fabric (131.71-m depth interval; PPL). (F) Cluster of small (50–100 μm) sphaerosiderite nodules exhibiting radial-concentric crystalline microstructures and characteristic sweeping extinction patterns (131.40-m depth interval; CPL).

TABLE 2. PEDOGENIC FEATURES OF THE NANUSHUK FORMATION, GRANDSTAND #1 CORE, NORTH SLOPE, ALASKA

Interval	Groundmass	Pedofeatures
171.34 m	Unit exhibits a crystallitic b-fabric groundmass. The Crystallitic domains are characterized by fine-silt and small patches of oriented clays (<10μm in size). The groundmass consists of 5–10% finely comminuted, opaque carbonaceous fragments. This unit is complexly mottled with crystallitic b-fabric domains interwoven with pervasively siderite-cemented domains.	Small (10–20 μm), equidimensional, siderite crystallites are ubiquitous in the groundmass.
171.90 m	Unit is characterized by stipple–speckled and striated b-fabric groundmass domains that are mottled together, having a contorted bedding appearance. Some of the speckled domains enveloped in striated b-fabric groundmass exhibit rounded, tubular, and prolate shapes possibly related to burrowing, and have lower hues and chromas. Porostriated b-fabrics are also noted around some planar voids (pores). The groundmass consists of up to 15% finely comminuted, opaque carbonaceous fragments.	Small (10–20 μm), equidimensional, siderite crystallites are ubiquitous in the groundmass. Dense aggregates of the siderite crystallites exhibit variable degrees of organization into spherical, nodular forms that are 100–500 μm in diameter. Some of the nodules exhibit crude concentric internal fabrics. Large (5-10 mm), irregular clusters of the nodular siderites are easily viewed at the macroscale as prominent moderate reddish brown (10R 4/6) mottles.
131.71 m	This unit is characterized by a stipple–speckled b-fabric groundmass. The groundmass consists of up to 15% finely comminuted, opaque carbonaceous fragments.	Small (10–20 μm) equidimensional, siderite crystallites are ubiquitous in the groundmass. Throughout much of the sample, the crystallites have aggregated into distinctly spherical forms (50–150 μm). Dense aggregates of the spherical forms were incorporated into larger, nodular forms that are 200–500 μm in diameter, some of which are well rounded. Some of the spherical aggregates (50–150 μm) exhibit crude concentric internal fabrics, and the boundaries of the individual crystallites are not discernable. Clusters of the spherical aggregates occur in linear arrays surrounding thin (10–20 μm), continuous, opaque, typic carbonaceous coatings. Spherical siderite aggregates are also arrayed along silty-clay laminae in a large (1 cm depth), dense, complete infilling.
131.40 m	This unit is characterized by a striated b-fabric groundmass. The groundmass consists of up to 10% finely comminuted, opaque carbonaceous fragments.	Small (10–20 μm) equidimensional, siderite crystallites are ubiquitous in the groundmass. Throughout much of the sample, the crystallites have aggregated into distinctly spherical forms (50–150 μm). In several areas of this unit, the spherical siderite aggregates have sustained textural reorganization to clearly radial-concentric crystalline microstructures exhibiting pseudo-uniaxial cross extinction in cross-polarized light. These siderite nodules are generally 50–100 μm in size, and have the characteristics of sphaerosiderites as defined by Ludvigson et al. (1998). Often the sphaerosiderites occur as peanut-shaped forms of two nodules coalesced in optical continuity. Dense clusters of the spherical siderite aggregates are observed surrounding kaolinite-filled voids (200–400 mm in diameter), and the sphaerosiderites occur on the inside of the cluster adjacent to the clay. Some sphaerosiderites are also observed in clusters or arrays associated with thin (<20 μm), discontinuous, typic carbonaceous coatings. Patches of densely packed spherical siderite aggregates were incorporated into larger, nodular forms that are up to 1 cm in diameter, and are easily seen at the macro-scale as brownish-red mottles. Some highly degraded, thin (<50 mm), discontinuous, typic argillaceous coatings exhibiting first order birefringence and diffuse extinction patterns are observed. The argillaceous coatings have been heavily reworked into the groundmass and may be the source of much of the clay particles generating the striated b-fabric.

depth interval has the most variable siderite compositions, ranging from 79.16 to 93.70 mol % $FeCO_3$. Substitutions of Ca^{2+} range from 2.12 to 6.54 mol % $CaCO_3$, Mg^{2+} ranges from 0.07 to 12.55 mol % $MgCO_3$, Mn^{2+} ranges from 1.63 to 12.09 mol % $MnCO_3$, and Sr^{2+} is less than 0.05 mol % $SrCO_3$.

DISCUSSION

The micromorphological characteristics suggest that the pedogenic horizons described above were formed in poorly developed soils, analogous to modern Inceptisols (Soil Survey Staff, 1998). The pedogenic horizons of the Nanushuk Formation in the Grandstand #1 core are characterized by gleyed colors, few fine root traces, abundant siderite, abundant organic fragments, rare clay and silty-clay coatings and infillings, and some preservation of primary sedimentary stratification. The gleyed colors and abundance of siderite and well preserved organic matter suggest prevalent reducing conditions and are indicative of poorly drained, hydromorphic soils (Landuydt, 1990; Driese et al., 1995; McCarthy et al., 1997; Ludvigson et al., 1998; McCarthy and Plint, 1999). The groundmass microfabrics reflect primary sedimentary structures, pedogenic modifications, and probably compaction (McCarthy and Plint, 1999). Striated b-fabrics are typically attributed to stresses involved with shrink swell processes in the soil (Brewer, 1976). Speckled b-fabrics are often produced from suspension settling and/or flocculation of fine materials during deposition (Bullock et al., 1985). The crystallitic b-fabrics are likely a result of the pervasive siderite formation and ferroan dolomite precipitation in the groundmass. The rare, highly degraded clay coatings indicate some translocation of clay particles through the soil profile. The few places where striated b-fabrics are noted may have resulted from clay coatings that were reworked into the matrix through reorganization of the soil (Fitzpatrick, 1993; McCarthy and Plint, 1999). This is further substantiated by slickensides noted at the macroscale. The silty-clay infillings may indicate translocation of material under higher-energy conditions and may signify wetter and possibly colder conditions (Fedoroff et al., 1990; Nettleton et al., 1994; McCarthy and Plint, 1999). The complex, contorted bedding in the lower units (171.34 and 171.19 m) may be primary sedimentary stratification that was disturbed through bio- and pedoturbation (shrink-swell) processes. The poikilotopic ferroan dolomite cements, and void filling sparry dolomites associated with the carbonaceous materials are interpreted to have been precipitated from later-diagenetic pore fluids. The presence (although rare) of degraded clay coatings, striated microfabrics, and pedogenic slickensides suggests that these paleosols were subjected to cyclic wetting and drying (McCarthy and Plint, 1998). Siderites likely formed during predominantly wet conditions. Thus, the paleosols may have had an early developmental

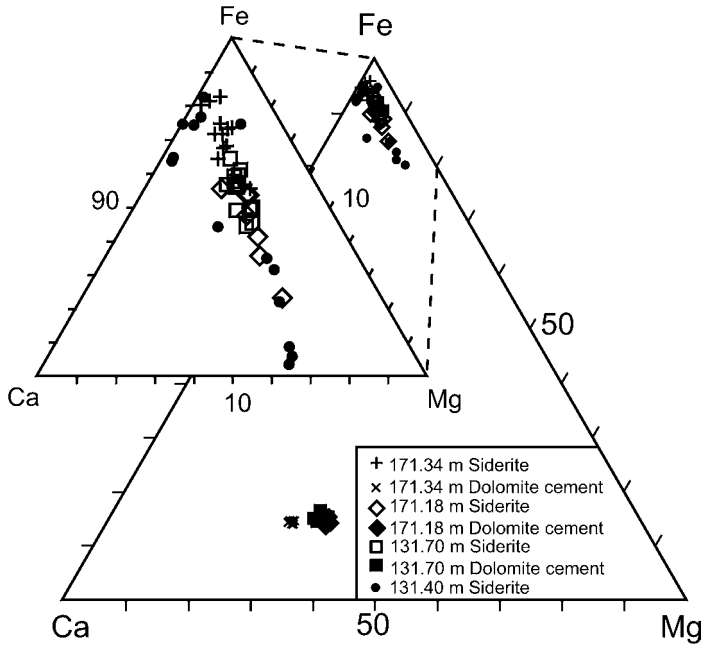

Figure 7. Composite ternary diagram showing relative Fe, Ca, and Mg compositions of paleosol siderites and ferroan dolomite cements.

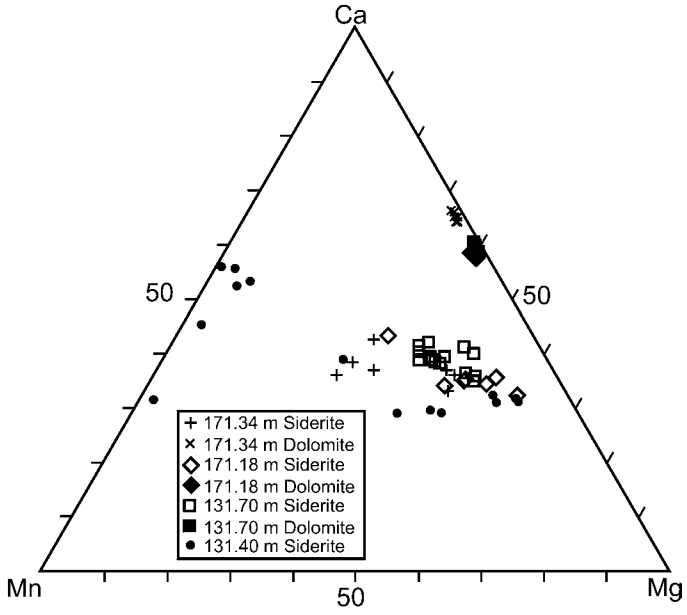

Figure 8. Composite ternary diagram showing relative Ca, Mn, and Mg compositions of paleosol siderites and ferroan dolomite cements.

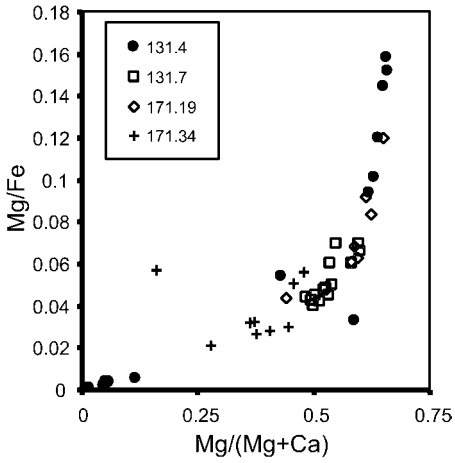

Figure 9. Plot illustrating paleosol siderite Mg/Fe ratios versus Mg/(Mg + Ca) ratios. For comparison, relatively pure paleosol sphaerosiderites (>95 mol % $FeCO_3$) from Boulder Creek Formations of British Columbia have Mg/Fe ratios on the order of 0.005, and Mg/(Mg + Ca) ratios on the order of 0.225.

stage characterized by wet dry cycles followed by late-stage hydromorphism (McCarthy and Plint, 1998, 1999).

The generally positive siderite $\delta^{13}C$ values suggest formation in wetland paleosols under reducing conditions in the methanogenic zone (Fig. 4). Methane is generated by anaerobic methanogenic bacteria in recent anoxic sediments by two metabolic pathways: acetate splitting (fermentation) and CO_2 reduction (Whiticar et al., 1986; Tucker and Wright, 1990; Schlesinger, 1997). During the process of CO_2 reduction, the CO_2 present as HCO_3^- serves as the electron acceptor (Schlesinger, 1997). The fractionation of ^{12}C and ^{13}C during the methane generation process is kinetically controlled, enriching the CH_4 in ''light'' ^{12}C and the residual CO_2 in ''heavy'' ^{13}C. Thus, the residual HCO_3^- in pore fluids during siderite precipitation was enriched in ^{13}C, resulting in the enriched (positive) $\delta^{13}C$ values (Whiticar and Faber, 1986).

Siderite is a very useful indicator of fluid chemistries during its precipitation because it forms under restricted redox conditions with low sulfide and high bicarbonate concentrations (Garrels and Christ, 1965; Hem, 1985). Siderite is a refractory carbonate mineral with no unstable polymorphs (Mozley and Carothers, 1992), and it generally does not undergo recrystallization and reequilibration typical of calcite under most diagenetic conditions (Matsumoto and Iijima, 1981; Curtis and Coleman, 1986; Mozley and Carothers, 1992). The compositional variations in the Nanushuk Formation siderites were probably influenced by fluid mixing processes during precipitation rather than by any later diagenetic alterations. Increased substitution of Ca^{2+} and Mg^{2+} and high siderite elemental Mg/Fe and Mg/(Ca + Mg) ratios likely resulted from mixing of modified marine fluids or brines with meteoric pore fluids during precipitation (Matsumoto and Iijima, 1981; Mozley, 1989) (Fig. 9). Introduction of significant volumes of marine-derived pore fluids would increase the SO_{4-}^{-2} concentrations in the pore fluids, thus favoring pyrite formation over siderite under conditions of sulfate reduction (Berner, 1981; Mozley and Carothers, 1992). The lack of sedimentary

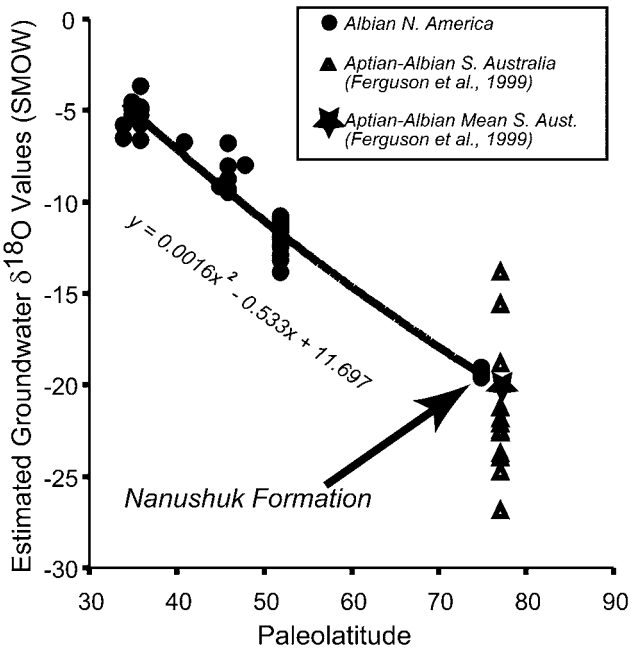

Figure 10. Estimated paleogroundwater δ18O values calculated from latitudinal gradient in meteoric sphaerosiderite δ18O values are plotted to show Late Albian trend in meteoric δ18O values for Cretaceous Western interior Basin and North Slope, Alaska (Ufnar et al., 2002). Also illustrated are high-paleolatitude groundwater δ18O values calculated from middle Cretaceous calcite cements in southern Australia from Ferguson et al. (1999).

pyrite, however, and the siderite δ13C compositions suggest reducing conditions had progressed to methanogenesis in meteoric-dominated fluids (Schlesinger, 1997).

The oxygen isotopic values preserved in the siderites of the Nanushuk Formation are strongly depleted (–17 to −14‰ PDB) and relatively invariant within individual horizons, with the exception of the 171.34-m depth interval (discussed below). The 171.19, 131.71, and 131.40 m horizons define MSLs (Ludvigson et al., 1998), suggesting precipitation from meteoric-phreatic fluids. Minor deviations in the oxygen isotopic compositions may be attributed to elemental substitutions in the siderite crystals, thus imparting some variable isotopic fractionation (Mozley and Carothers, 1992) and intrinsic variations in groundwater δ18O values and MAT over time. The strongly depleted compositions are consistent with North American paleolatitudinal trends in Albian paleoprecipitation δ18O values and provide the northern tie-point for our paleolatitudinal reconstructions (Ludvigson et al., 1998; Ufnar et al., 2002) (Fig 10). Calculated paleogroundwater and paleoprecipitation δ18O values range between −23.0 and −19.5‰ SMOW on the North Slope (Fig. 5). Our calculations are consistent with the groundwater δ18O values calculated from the oxygen isotopic values of calcite cements in high-paleolatitude, middle Cretaceous deposits of southern Australia (Ferguson et al., 1999). These highly depleted δ18O compositions probably resulted from globally increased precipitation due to an intensified hydrologic cycle during the ''greenhouse-world'' conditions of the middle Cretaceous (Ludvigson et al., 1998; White et al., 2001; Ufnar et al., 2002).

The elemental data discussed above suggest precipitation from mixed meteoric- and marine-phreatic fluids, and the covariant δ18O versus δ13C trend in the 171.34-m depth interval further supports this interpretation (Carpenter et al., 1988; Lohmann, 1988). Mixing hyperbolas were calculated using mass balance equations to mix fluids of differing total dissolved carbon (ΣCO_2) values, δ13C of dissolved inorganic carbon (ΣCO_2), and δ18O water to depict hyberbolic fluid mixing trends yielding a range of possible siderite compositions. Two hyperbolic mixing curves constraining the covariant siderite δ18O versus δ13C compositional trend in the 171.34-m depth interval were calculated between two end-member fluids, meteoric phreatic fluids, and modified marine phreatic fluids. The modified marine-phreatic end-member is enriched in 18O, 13C, and ΣCO_2 with values of −1.0‰ (SMOW), +11.0‰ (PDB), and the CO_2 (ΣCO_2) concentration was set to be 3.0 mmoles/l (seawater ΣCO_2 values range from 2.0 to 3.0 mmoles/l). The depleted meteoric-phreatic end-member δ18O water composition is −18.0‰ (SMOW) and the δ13C dissolved inorganic carbon (DIC) compositions range between −2.0‰ and +5.0‰ (PDB) with ΣCO_2 concentrations ranging between 0.35 and 0.50 mmoles/l, respectively. The calculated siderite δ18O and δ13C values that would precipitate from variable mixtures of these fluids are illustrated in Figure 11 (mixtures 1 and 2 curves). The siderite δ18O values range between –16.71‰ and −0.84‰ (PDB), and the δ13C compositions range between +13.82‰ (PDB) and +1.20‰ (mixture 1) and +8.22‰ (PDB) (mixture 2).

The hyperbolic trends modeled for the 171.34-m depth interval present a range of possible fluid compositions that might explain the covariant δ18O versus δ13C trend. Both end-member fluids were strongly reducing (low Eh), and the modeled mixing curves suggest that the diagenetic fluid was less than 25% seawater. The depleted end-member compositions most closely resemble the meteoric groundwater compositions and are consistent with the MSLs obtained from the other horizons. The enriched compositions represent products from proportionally higher concentrations of modified marine-phreatic fluids.

Siderites in the pedogenic horizons of the Nanushuk Formation have proved to be a critical link in our efforts to reconstruct the latitudinal δ18O gradients of precipitation for the equable middle Cretaceous (Ludvigson et al., 1998; Ufnar et al., 2002). A stable isotope mass balance model of the middle Cretaceous hydrologic cycle developed by our research group compares hemispherical precipitation fluxes in simulations of the modern versus Albian worlds (Ufnar et al., 2002). The dimensionless fractions expressing the precipitation fluxes can be parameterized to calculate estimates of precipitation rates (see details presented in Ufnar et al., 2002).

Precipitation isotopic data from the International Atomic Energy Agency/World Meteorological Organization (IAEA/WMO) Barrow, Alaska, station located at 71.3° N latitude (Rozanski et al., 1993) provides modern climatological information that can be used to derive estimates of precipitation rates. Long-term historic records from Barrow, Alaska, indicate a MAT of −12.7 °C, a precipitation rate of 133 mm/yr, and a weighted mean precipitation δ18O composition of −19.61‰ (SMOW). Calculations of saturation vapor pressures comparing the modern Barrow, Alaska, MAT of−12.7 °C to the ancient Albian North Slope empirical estimates of 10 °C (Parrish and Spicer, 1988a, b) suggest a 343% increase in the vapor-holding capacity of the

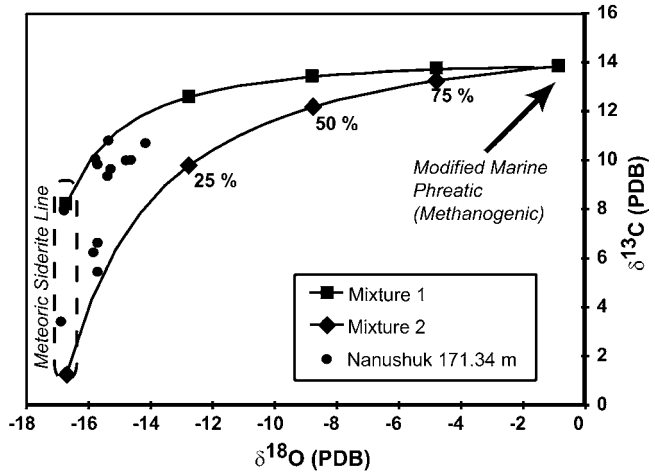

Figure 11. Graph illustrating results of fluid mixing model that generates hyperbolic fluid mixing trends of possible isotopic values ranging between meteoric phreatic and modified marine phreatic end-member compositions. Curves were modeled to envelop range of empirical siderite values. Square and diamond symbols represent 25, 50, and 75% fluid mixtures, and thus show that 171.34-m depth interval siderite values resulted from fluid mixtures that were less than 25% seawater. Moreover, both end-member fluids had DIC values that were strongly controlled by anaerobic methanogenesis.

local middle Cretaceous atmosphere compared to today. Following the calculation procedures outlined in Ufnar et al. (2002), a precipitation rate of 485 mm/yr has been estimated for the North Slope during the late Albian. With increased paleotemperature, the precipitation rate would be expected to increase (e.g., MAT of 14 °C = 626 mm/yr).

These estimates are consistent with precipitation rates required for modern peat formation, which are constrained by both temperature and precipitation (Lottes and Ziegler, 1994). Sustained annual rainfall is required to provide enough water to support vegetation and maintain a stable high water table inhibiting organic matter decay, and cooler temperatures are important for reducing evaporation rates (Lottes and Ziegler, 1994). The peat prediction maps of Lottes and Ziegler (1994) suggest that 10 °C is a temperature minimum, because growth in plants generally occurs during months exceeding this temperature (Walter, 1985). Furthermore, Lottes and Ziegler (1994) concluded that monthly rainfall rates of 40 mm or more for most of the year are necessary to sustain peat development. This monthly rate corresponds to 480 mm/yr, which agrees very well with our calculated rates for the Albian. These mutually compatible conclusions help explain the formation of lignite at high latitudes in the Nanushuk Formation strata of the North Slope, Alaska.

CONCLUSIONS

Pedogenic siderites from the North Slope Alaska are pivotal to our paleoclimatological reconstructions of the equable middle Cretaceous of North America. They provide a critical high-paleolatitude proxy for determining latitudinal gradients in paleoprecipitation $\delta^{18}O$ compositions.

The impure siderite compositions (<95 mol% $FeCO_3$), with increased substitution of Ca, Mg, Mn, and Sr, and high Mg/Fe and Mg/(Ca + Mg) ratios suggest marine influences on pore fluid compositions during siderite precipitation. Marine influence is further substantiated by the covariant $\delta^{18}O$ versus $\delta^{13}C$ trend at the 171.34-m depth interval. A fluid mixing model was used to generate two hyperbolic fluid mixing curves that envelop the empirical data. The end-member fluids have compositions ranging between an enriched modified marine-phreatic composition and a depleted meteoric-phreatic composition. Mass balance modeling experiments suggest that the diagenetic fluids were predominantly meteoric in origin and were always less than 25% seawater.

Calculations of precipitation rates for the Late Albian of the North Slope (485 mm/yr) are entirely consistent with the precipitation rates necessary to maintain modern peat-forming environments (Lottes and Ziegler, 1994). These calculations further reinforce the empirical paleotemperature estimates of Parrish and Spicer (1988) and the modeled precipitation fluxes of Ufnar et al. (2002). This information can be used to advance global circulation modeling experiments of ''greenhouse-world'' climates to further understanding of polar warmth and precipitation rates in simulations of global climate systems with decreased equator-to-pole temperature gradients.

ACKNOWLEDGMENTS

We are grateful to the University of Iowa Center for Global and Regional Environmental Research for a student research grant award made to the senior author that provided much of the funding for this project. Additional support was provided by the University of Iowa Department of Education GAANN fellowship. We thank Scott J. Carpenter for supervising the stable isotope laboratory and for providing helpful advice. We thank Bob Ravn (Aeon Biostratigraphic Services, Anchorage, Alaska) for identifying palynomorphs. We thank Peter McSwiggen for his assistance at the University of Minnesota Electron Microprobe Laboratory. We thank the personnel at the U.S. Geological Survey core research laboratory in Denver, Colorado, and Dave Houseknecht and the other the directors of the U.S. Geological Survey National Petroleum Reserve Alaska (NPR-A) core workshop in Denver (1999). We also thank Paul McCarthy and Gregory Retallack for their very helpful and thorough reviews of this manuscript.

REFERENCES CITED

Ahlbrandt, T.S., 1979, Preliminary geologic, petrologic, and paleontologic results of the study of Nanushuk Group rocks, North Slope, Alaska: U.S. Geological Survey Circular 794, 163 p.

Barron, E.J., Hay, W.W., and Thompson, S., 1989, The hydrologic cycle: a major variable during Earth history: Paleogeography, Paleoclimatology, Palaeoecology, v. 75, p. 157–174.

Barron, E.J., Fawcett, P.J., Peterson, W.H., Pollard, D., and Thompson, S.L., 1995, A ''simulation'' of middle Cretaceous climate: Paleoceanography, v. 10, no. 5, p. 953–962.

Barron, E.J., and Washington, W.M., 1982, Cretaceous climate: a comparison of atmospheric simulations with the geologic record: Palaeogeography, Palaeoclimatology, Palaeoecology, v. 40, p. 103–133.

Berner, R.A., 1981, A new classification of sedimentary environments: Journal of Sedimentary Petrology, v. 51, p. 359–365.

Bullock, P., Fedoroff, N., Jongerius, A., Stoops, G., Tursina, T., and Babel, U., 1985, Handbook for soil thin section description: England, Waine Research Publications, 152 p.

Brewer, R., 1964, Fabric and Mineral Analysis of Soils: New York, John Wiley and Sons470 p.

Brewer, R., 1976, Fabric and Mineral Analysis of Soils: New York, Krieger Publishing, 482 p.

Carothers, W.W., Lanford, H.A., and Rosenbauer, R.J., 1988, Experimental oxygen isotope fractionation between siderite-water and phosphoric acid liberated CO2-siderite: Geochimica et Cosmochimica Acta, v. 52, p. 2445–2450.

Carpenter, S.J., Erickson, M.J., Lohmann, K.C., and Owen, M.R., 1988, Diagenesis of fossiliferous concretions from the Upper Cretaceous Fox Hills Formation, North Dakota: Journal of Sedimentary Petrology, v. 52, p. 792–814.

Curtis, C.D., and Coleman, M.L., 1986, Controls on the

precipitation of early diagenetic calcite, dolomite, and siderite concretions in complex depositional sequences, in Gautier, D.L., ed., Roles of organic matter in sediment diagenesis: Society of Economic Paleontologists and Mineralogists Special Publication 38, p. 23–33.

Douglas, R.G., and Savin, S.M., 1975, Oxygen and carbon isotopic analyses of Tertiary and Cretaceous microfossils from Shatsky Rise and other sites in the North Pacific Ocean, *in* Larson, R.L., and Moberly, R., Bukry, D., Foreman, H.P., Gardner, J.V., Keene, J.B., Lancelot, Y., Luterbacher, H., Marshall, M.C., and Matter, A., eds., Initial Reports of the Deep Sea Drilling Project, Volume 32: Washigton, D.C., U.S. Government Printing Office, p. 509–520.

Driese, S.G., Simpson, E.L., and Eriksson, K.A., 1995, Redoximorphic paleosols in alluvial and lacustrine deposits, 1.8 Ga Lochness Formation, Mount Isa, Australia: pedogenic processes and implications for paleoclimate: Journal of Sedimentary Research, v. A65, p. 675–689.

Fassell, M.L., and Bralower, T.J., 1999, Warm, equable middle Cretaceous: Stable isotope evidence, *in* Barrera, E., and Johnson, C.C., eds., Evolution of the Cretaceous Ocean-Climate System: Boulder, Colorado, Geological Society of America Special Paper 332, p. 121–142.

Fedoroff, N., Courty, M.A., and Thompson, M.L., 1990, Micromorphological evidence of paleoenvironmental change in Pleistocene and Holocene paleosols, in Douglas, L.A., ed., Soil Micromorphology: A Basic and Applied Science: Amsterdam, Elsevier, p. 653–656.

Ferguson, K.M., Gregory, R.T., and Constantine, A., 1999, Lower Cretaceous (Aptian-Albian) secular changes in the oxygen and carbon isotope record from high paleolatitude, fluvial sediments, southeast Australia: Comparisons to the marine record, *in* Barrera, E., and Johnson, C.C., eds., Evolution of the Cretaceous Ocean-Climate System: Boulder, Colorado, Geological Society of America Special Paper 332, p. 59–72.

Fitzpatrick, E.A., 1993, Soil Microscopy and Micromorphology: New York, John Wiley and Sons, 304 p.

Garrels, R.M., and Christ, C.L., 1965, Minerals, Solutions, and Equilibria: New York, Harper and Row, 450 p.

Harrington, J.B., 1987, Climatic Change: A review of causes: Canadian Journal of Forest Research, v. 11, p. 1313–1339.

Hem, J.D., 1985, Study and interpretation of the chemical characteristics of natural waters: U.S. Geological Survey Water Supply Paper 2254, 263 p.

Huber, B.T., Hodell, D.A., and Hamilton, C.P., 1995, Mid- to Late Cretaceous climate of the southern high latitudes: stable isotopic evidence for minimal equator-to-pole thermal gradients: Geological Society of America Bulletin, v. 107, p. 1164–1191.

Huber, B.T., Norris, R.D., and MacLeod, K.G., 2002, Deep-sea paleotemperature record of extreme warmth during the Cretaceous: Geology, v. 30, p. 123–126.

Huffman, A.C., Jr., 1985, Introduction to the Geology of the Nanushuk Group and Related Rocks, North Slope, Alaska, in Huffman, A.C., Jr., ed., Geology of the Nanushuk Group and Related Rocks, North Slope, Alaska: U.S. Geological Survey Bulletin B-1614, p. 1–6.

Landuydt, C.J., 1990, Micromorphology of iron minerals from bog ores of the Belgian Campine area, in Douglas, L.A., ed., Soil Micromorphology: A basic and applied science: Amsterdam, Elsevier, Developments in Soil Science, v. 19, p. 289–294.

Lloyd, C.R., 1982, The middle Cretaceous Earth: Paleogeography, ocean circulation, temperature, and atmospheric circulation: Journal of Geology, v. 90, p. 393–413.

Lohmann, K.C., 1988, Geochemical patterns of meteoric diagenetic systems and their application to studies of paleokarst, in James, N.P., and Choquette, P.W., eds., Paleokarst: Springer Verlag, p. 58–80.

Lottes, A.L., and Ziegler, 1994, World peat occurrence and the seasonality of climate and vegetation: Palaeogeography, Palaeoclimatology, Palaeoecology, v. 106, p. 23–37.

Ludvigson, G.A., Gonzalez, L.A., Metzger, R.A., Witzke, B.J., Brenner, R.L., Murillo, A.P., White, T.S., 1998, Meteoric sphaerosiderite lines and their use for paleohydrology and paleoclimatology: Geology, v. 26, p. 1039–1042.

Matsumoto, R., and Iijima, A., 1981, Origin and diagenetic evolution of Ca-Mg-Fe carbonates in some coalfields of Japan: Sedimentology, v. 28, p. 239–259.

McCarthy, P.J., and Plint, A.G., 1998, Recognition of interfluve sequence boundaries: Integrating paleopedology and sequence stratigraphy: Geology, v. 26, p. 387–390.

McCarthy, P.J., and Plint, A.G., 1999, Floodplain paleosols of the Cenomanian Dunvegan Formation, Alberta and British Columbia, Canada: Micromorphology, pedogenic processes, and paleoenvironmental implications, *in* Marriott, S.B., and Alexander, J., eds., Floodplains: Interdisciplinary Approaches: Boulder, Colorado, Geological Society of America Special Paper 163, p. 289–310.

McCarthy, P.J., Martini, I.P., and Leckie, D.A., 1997, Anatomy and evolution of a Lower Cretaceous alluvial plain: sedimentology and paleosols in the upper Blairmore Group, southwestern Alberta, Canada: Sedimentology, v. 44, p. 197–220.

Mozley, P.S., 1989, Relation between depositional environment and the elemental composition of early diagenetic siderite: Geology, v. 17, p. 704–706.

Mozley, P.S., and Carothers, W.W., 1992, Elemental and isotopic composition of siderite in the Kuparuk Formation, Alaska: effect of microbial activity and water/sediment interaction on early pore-water chemistry: Journal of Sedimentary Research, v. 62, no. 4, p. 681–692.

Molenaar, C.M., 1985, Subsurface correlations and depositional history of the Nanushuk Group and related strata, North Slope, Alaska, *in* Huffman, A.C., Jr., ed., Geology of the Nanushuk Group and Related Rocks, North Slope, Alaska: U.S. Geological Survey Bulletin B-1614, p. 37–59.

Mull, C.G., 1985, Cretaceous tectonics, depositional cycles, and the Nanushuk Group, Brooks Range and Arctic Slope, Alaska, *in* Huffman, A.C., Jr., ed., Geology of the Nanushuk Group and Related Rocks, North Slope, Alaska: U.S. Geological Survey Bulletin B-1614, p. 7–36.

Mull, C.G., Houseknecht, D.W., and Bird, K.J., 2003, Revised Cretaceous and Tertiary Stratigraphic Nomenclature in the Colville Basin, Northern Alaska: U.S. Geological Survey Professional Paper 1673, 51 p.

Mutterlose, J., 1992, Biostratigraphy and paleobiogeography of Early Cretaceous calcareous nanofossils: Cretaceous Research, v. 18, p. 167–189.

Nettleton, W.D., Brasher, B.R., Baumer, O.W., and Darmody, R.G., 1994, Silt flow in soils, *in* Ringrose-Voase, A.J., and Humphreys, G.S., eds., Soil Micromorphology: Studies in Management and Genesis: Amsterdam, Elsevier, 361–372.

O'Sullivan, P.B., 1999, Thermochronology, denudation and variations in palaeosurface temperature: a case study from the North Slope foreland basin, Alaska: Basin Research, v. 11, p. 191–204.

Parrish, J.T., and Spicer, R.A., 1988a, Middle Cretaceous woods from the Nanushuk Group, central North Slope, Alaska: Paleontology, v. 31, p. 19–34.

Parrish, J.T., and Spicer, R.A., 1988b, Late Cretaceous vegetation of the North Slope, Alaska: a near polar temperature curve: Geology, v. 16, p. 22–25.

Poulsen, C.J., Barron, E.J., Johnson, C., and Fawcett, P., 1999, Links between major climatic factors and regional oceanic circulation in the middle Cretaceous, *in* Barrera, E., and Johnson, C.C., eds., Evolution of the Cretaceous Ocean-Climate System: Boulder, Colorado, Geological Society of America Special Paper 332, p. 73–90.

Rozanski, K., Araguas-Araguas, L., Gonfiantini, R., 1993, Isotopic patterns in modern global precipitation, *in* Swart, P.K., Lohmann, K.C., McKenzie, J., and Savin, S., eds., Climate Change in Continental Isotopic Records: American Geophysical Union Geophysical Monograph 78, p. 1–36.

Schlesinger, W.H., 1997, Biogeochemistry, An Analysis of Global Change, Second Edition: San Diego, California, Academic Press, 588 p.

Sloan, L.C., and Barron, E.J., 1990, ''Equable'' climates during Earth history?: Geology, v. 18, p. 489–492.

Soil Survey Staff, 1998, Keys to Soil Taxonomy, Eighth Edition: U.S. Department of Agriculture, Natural Resources Conservation Service, http://www.pedosphere.com/resources/sg_usa/.

Spicer, R.A., and Corfield, R.M., 1992, A review of terrestrial and marine climates in the Cretaceous with implications for modeling the ''Greenhouse Earth'': Geological Magazine v. 129, p. 169–180.

Spicer, R.A., and Parrish, J.T., 1986, Paleobotanical evidence for cool north polar climates in middle Cretaceous (Albian-Cenomanian) time: Geology, v. 14, p. 703–706.

Spicer, R.A., and Parrish, J.T., 1990a, Latest Cretaceous woods of the central North Slope, Alaska: Paleontology, v. 33, pt. 1, p. 225–242.

Spicer, R.A., and Parrish, J.T., 1990b, Late Cretaceous-early Tertiary palaeoclimates of northern high latitudes: a quantitative view: Journal of the Geological Society, London, v. 147, p. 329–341.

Tucker, M.E., and Wright, V.P., 1990, Carbonate Sedimentology: London, Blackwell Scientific Publications, 482 p.

Ufnar, D.F., Gonzalez, L.A., Ludvigson, G.A., Brenner, R.L., Witzke, B.J., 2001, Stratigraphic implications of meteoric sphaerosiderite $\delta^{18}O$ compositions in paleosols of the Cretaceous (Albian) Boulder Creek Formation, NE British Columbia Foothills, Canada: Journal of Sedimentary Research, v. 71, p. 1017–1028.

Ufnar, D.F., González, L.A., Ludvigson, G.A., Brenner, R.L., and Witzke, B.J., 2002, The middle Cretaceous water bearer: Isotope mass balance quantification of the Albian hydrologic cycle: Palaeogeography, Palaeoclimatology, Palaeoecology, v. 188, p. 51–71.

Walter, H., 1985, Vegetation of the Earth: Berlin, Springer-Verlag, 318 p.

White, T.S., Witzke, B.J., Ludvigson, G.A., Brenner, R.L., Gonzalez, L.A., Ravn, R.L., 2000a, The paleoclimatological significance of Albian (middle Cretaceous) sphaerosiderites from eastern Saskatchewan and western Manitoba: Summary of Investigations 2000, volume 1: Saskatchewan Geological Survey Miscellaneous report 2000–4.1, p. 63–75.

White, T.S., Witzke, B.J., and Ludvigson, G.A., 2000b, Evidence for an Albian Hudson arm of the North American Cretaceous Western Interior Seaway: Geological Society of America Bulletin, v. 112, p. 1342–1355.

White, T.S., Gonzalez, L.A., Ludvigson, G.A., Poulsen, C., 2001, Middle Cretaceous greenhouse hydrologic cycle of North America: Geology, v. 29, p. 363–366.

Whiticar, M.J., and Faber, E., 1986, Methane oxidation in seawater and water column environments—isotopic evidence: Organic Geochemistry, v. 10, p. 759–768.

Whiticar, M.J., Faber, E., and Schoell, M., 1986, Biogenic methane formation in marine and freshwater environments: CO_2 reduction vs. acetate fermentation—isotopic evidence: Geochimica Cosmochimica Acta, v. 50, p. 693–709.

Wolfe, J.A., 1971, Tertiary climatic fluctuations and methods of analysis of Tertiary climates in the Northern Hemisphere: Palaeogeography, Palaeoclimatology, Palaeoecology, v. 9, p. 27–57.

Wolfe, J.A., 1979, Temperature parameters of humid to mesic forests of eastern Asia and relationships to forests of other regions of the Northern Hemisphere and Australasia: U.S. Geological Survey Professional Paper 1106, 37 p.

Wolfe, J.A., and Upchurch, G.R., 1987, North American nonmarine climates and vegetation during the Late Cretaceous: Palaeogeography, Palaeoclimatology, Palaeoecology, v. 61, p. 33–77.

MANUSCRIPT RECEIVED BY THE SOCIETY 8 NOVEMBER 2002
REVISED MANUSCRIPT RECEIVED 24 JULY 2003
MANUSCRIPT ACCEPTED 14 AUGUST 2003

Printed in the USA